Embodied carbon of structural earthen composites with natural materials and byproducts suitable for robotic 3d printing

Mohamad Fouad Hanifa[1,*], *Harish* Daruari[2,**], *Bruno* Figueiredo[3,***], and *Paulo* Mendonça[4,****]

[1,2,3,4] School of Architecture, Art, and Design (EAAD), Lab2PT, Portugal
*Mohamad.fouad.nader.hanifa@iaac.net, **harish.daruari@gmail.com, ***bfigueiredo@eaad.uminho.pt,
****mendonca@eaad.uminho.pt

Abstract. The objective of this research is focused on 3D printing techniques using natural materials in the construction sector. Digital fabrication has captured widespread attention for its remarkable ability to craft parametric and complex geometry with relative ease. Beyond its technical prowess, this process holds great potential in addressing two pressing issues: waste management and carbon emissions, to reduce costs and environmental impacts. This study assesses the eco-efficiency of 3D printing with earthen composites compared to conventional construction materials in large-scale Robotic fabrication, employing the life cycle assessment (LCA) framework to quantify the environmental impacts of materials suitable for 3D printing. An eco-efficiency analysis was employed to aggregate the results of LCA into a single framework to assist in decision-making by selecting the most optimized and eco-efficient alternative. The findings indicate that shell structures built using additive manufacturing and 3D printed materials can be better optimized for efficiency. This paper comprehensively examines 3D printing with earth materials, focusing particularly on biocomposites, byproducts, and direct extrusion printing methods. Comparative analysis highlights the materials, processes, and industries driving these advancements. There has been a surge of interest in reinforcing 3D-printed structures with natural fibres and additives. A significant aspect of this study explores how 3D printing, especially when utilizing natural materials and byproduct-based composites, can contribute positively to the environment.

1 Introduction

The contemporary age has been shaped by a "growth model" with productivity serving as one of its key foundations. Driven by the need to keep pace with a rapidly expanding global population, industries have constantly pursued enhancing their processes. This quest for efficiency has significantly impacted the construction industry, which accounts for nearly 40% of yearly human-induced greenhouse gas emissions (GHG). Within this framework, the rise of additive manufacturing technologies including 3D printing (3DP) can largely be attributed to the demand for greater productivity. Moreover, these technologies are indicated for their ability to facilitate mass customization in architectural design nonetheless the employment of digital fabrication with concrete may lead to building components that possess a greater environmental impact compared to those produced through traditional construction methods [1]. Research indicates that the environmental footprint of one cubic meter of 3D-printed concrete is nearly double that of a cubic meter of conventionally cast concrete. This increased impact is dual: first, because the 3D-printed material itself is substantially heavier on the environment than the traditional one, and second 3D printing process consumes more energy during material deposition. Hence the ecological advantages of integrating additive manufacturing in construction are only realized when it results in significant savings on materials while the printing process maintains a low level of energy consumption [2]. In efforts to integrate digitalization with environmental sustainability, there has been a notable surge in research and practice aimed at employing low-carbon materials in additive manufacturing processes. Examples of such advancements include the substitution of geopolymer for epoxy-based resins in binder jetting methodologies as highlighted [3]. The adoption of low-carbon concrete in 3D printing is reported [4]. There are recent explorations into using earth-based matrices in conjunction with robotic manufacturing [5]. Despite these strides, the majority of research primarily concentrates on reducing the carbon footprint of the materials themselves, with less attention given to the embodied emissions associated with the manufacturing processes, and a comprehensive review of the literature has revealed that these process-related emissions are significant and cannot be overlooked. For instance, in traditional construction methods, material contributions to the overall lifecycle emissions average around 80%, with processing accounting for about 20%. Conversely, in the additive manufacturing techniques, this ratio is significantly reversed, emphasizing the need for a holistic approach to sustainability in digital fabrication processes [6].

This paper aims to undertake a comparative assessment of the environmental impacts associated with an array of earth-based compositions encompassing both traditional and innovative digital techniques. The Traditional methods under review include rammed earth and cob, while digital fabrication techniques will primarily focus on 3D printing (3DP) using earth-based composites as the primary construction material. The study focuses on evaluating the embodied carbons of the developed earth-based compositions, with an exclusive emphasis on carbon emissions and a comprehensive analysis of other environmental factors, such as (GWP) Global warming potential. It is essential to note that the study is specifically contextualized within Portugal and Spain, and its findings may not be universally applicable due to regional disparities in energy availability and material resources. The research delves into various aspects of 3DP with earth-based materials by exploring different parameters, including mix design proportions, presence of binders and, stabilizers. According to existing literature, the speeds of earth-based 3DP processes typically range between 20-50 mm/s, which is slower compared to concrete-based printing [7]. The layer thickness ranges from 0.01 to 0.04m. These discrepancies in operational parameters can be attributed to the distinct physical and rheological characteristics of earth and concrete materials [8,9].

2 Motivation and related work

2.1 Motivation and related work

Humans have used soil for construction since the earliest shelters were built. Today an estimated 1 to 3 thousand million people inhabit buildings made from earth, and construction techniques using earth have diversified and advanced leading to energy-efficient and strong multi-story buildings in various regions around the globe. The urgent need for sustainable, low-carbon building materials to address climate change has made these earth-based methods align with international goals and local environmental strategies through current research. Using natural rammed earth and compressed earth blocks greatly reduces carbon footprint compared to concrete, serving well for non-load-bearing elements while providing increased thermal insulation. Even load-bearing earth structures have been successfully erected with some buildings in Yemen reaching up to ten stories constructed by materials exhibiting considerable compressive strength.

Despite these advantages, international building codes rarely reflect earth-based techniques, and there are some exceptions such as in Australia, New Zealand, and specific places like New Mexico, Zimbabwe, France, and Germany where regulations include earth constructions to varying extents. The major roadblock in standardizing these methods is the shortage of comprehensive engineering studies to quantify building performance. Furthermore traditional perceptions dismiss the earth as an ancient building medium, hindering its acceptance in modern construction [10,11]. However, with the arrival of 3D printing technology, a fresh, contemporary perspective is emerging.

This innovation carries the potential to transform attitudes towards earth construction by demonstrating its viability and encouraging wider adoption of eco-friendly building practices like rammed earth and compressed earth block construction. Despite examples of earthen buildings up to 10 stories and promising compressive strengths between 1 to 4 MPa, the widespread adoption of earth is hindered by misconceptions of it being outdated, but innovations like 3D printing could change this view and promote its use in contemporary construction [12].

2.2 Positioning

Place Rammed earth construction a practice with ancient roots is undergoing modern transformation through automation. Researchers are employing computer-aided pneumatic equipment and production lines to create prefabricated earth modules. An architectural project by Herzog and De Meuron and Martin Rauch embodies this innovation with its pre-made rammed earth walls. Similarly, advances in compressed earth block production feature mechanized compression systems enabling the fast creation of consistent, dense bricks [13,14].

Other explorations into digital fabrication have been conducted, such as using daubed wicker techniques and impact Printing, which involves moulding or piling wet earth in a manner reminiscent of traditional methods. Moreover, earth construction has embraced large-scale additive manufacturing (LSAM), also known as Contour Crafting. 3D-printed earth structures have risen across Italy, Spain, USA, and Dubai, marking a significant step in sustainable building practices. Research into this domain has focused on material processing and mechanical properties of these printed earth structures, highlighting their practical compressive strengths and potential additives like lime, cement, and natural fibers. Specific studies have probed the material and structural capacities of lime-enhanced earthen mixtures used by the Italian company WASP, revealing promising strength outcomes [15,16].

Recent investigations by Faleschini provide deeper insights into the effects of various stabilizers and fibers on engineered soil composites, scrutinizing their fresh properties and strength after different curing periods, which delves into the necessary rheology and chemistry for successful earth 3D printing. Noting a shift towards heavily processed materials improved by geopolymers, and plasticizing agents with research goes beyond mere materials considering the environmental impact with life cycle analysis, emphasizing the importance of sustainability in this evolving field [17].

The application of geopolymers in earth construction is suggested to enhance sustainability but detailed carbon footprint data for the process is not provided, and a comparison of suitable soils for earth 3DP focuses on their flow characteristics including multiple tests, unlike the single test reports. Despite existing full-scale, load-bearing 3D-printed earth structures, the specific mechanical properties of the materials are generally not detailed, revealing a gap in research on the durability of constructions made from minimally processed, local soils rather than engineered printing mixtures.

Research on the use of alginate to boost the initial strength of soil mixtures, enable taller structures within a single print with a study that explores the structural capacity of 3D-printed Earth (3DPE) by testing different wall designs, informed by the actual strength of printed cob samples averaging 0.87 MPa. Another study assesses the insulation properties of different soils used in 3D-printed cob, finding thermal conductivities comparable to traditional earthen materials and more efficient than 3DP with mortar or cast concrete [18]. In a unique single test, lime and sand enhance the earth mixture, with the test conducted on a hollow wall design with diagonal infills, this study compares these varied previous research findings and acknowledges the infancy of 3DPE research and one of its pivotal aims is to identify and recommend the most practical and applicable material testing approaches that suit standardized protocols, catering to the diverse climates and settings where earth buildings are viable [19].

2.3 Material Formulation / Additives

Numerous studies have examined the material properties of soils for raw earth construction. However, global surveys and current building codes rarely provide comprehensive guidelines, except in regions like New Zealand, Australia, Germany, and New Mexico, where stabilizers like cement are recommended to meet structural requirements. Research indicates that particle size, fiber content, and clay amount significantly affect the compressive strength and durability of earth mixtures, potentially reducing the need for cement and preserving environmental benefits. Studies suggest that increasing fiber content in compressed earth can achieve strength comparable to adding 1-2% cement. The challenge is to enhance the structural performance of earthen materials while maintaining a low carbon footprint [20,21].

Introducing cement, even in small amounts, to traditional earthen elements like Compressed Earth Blocks (CEB) or rammed earth, can inadvertently lead to a carbon impact comparable to conventional concrete constructions, due to the inherently thick walls of earthen structures. Additionally, once the cement is incorporated, the earth material loses its recyclability [22]. Our study does not propose a one-size-fits-all solution for all types of earth construction but rather adheres to up-to-date best practices identified in scholarly research, including earth-based composite optimization for a minimal embodied carbon with best mechanical strength performance.

3 Methods

The imperative of selecting, processing, and characterizing materials poses significant challenges in the domain of earthen architecture, attributable to the inherent heterogeneity of indigenous material sources, and these challenges echo within 3DP technological systems, encompassing a spectrum from desktop applications to full-scale construction implementations within the absence of uniform protocols for material processing and calibration precludes the realization of highly precise and functional geometric outputs via printing. Consequently, a majority of 3DP apparatuses necessitate the utilization of precisely engineered materials, encompassing moisture-regulated thermoplastics to expeditiously solidify mortars, customarily synthesized by industrial entities for compatibility with specialized extrusion mechanisms while In the context of architectural applications, the integration of additive manufacturing presents substantial obstacles and the specialized mixtures requisite for 3DP are notably cost-intensive and suffer from erratic availability within The paradigm of reinforced concrete stands as a quintessential model of a scalable construction technology predicated on abundantly available, local materials, amenable to in situ calibration with additives such as sand, gravel, and water, Within the purview of this research, we conduct a scrutinization of extant methodologies germane to the enhancement of earth as a functional medium for Large-Scale Additive Manufacturing (LSAM).

Concurrently, we introduce innovative, site-specific assessment techniques aimed at expediting the material evaluation and modification processes, and this encompasses the experimental printing of earth cylinders, the development of novel volumetric measurement methodologies, and preliminary hydrostatic pressure experimentation designed to evaluate the applicability of 3D-printed earth. Additionally, we delineate a methodological framework for the Life Cycle Analysis (LCA) specific to 3D-printed earthen constructs to advance the premise that for LSAM, or digital fabrication more broadly, to achieve widespread adoption in construction paradigms, also the computational and mechanical infrastructures must evolve to accommodate ecologically sourced materials as shown in Fig.1 which this study contributes foundational research aimed at such an evolution, potentially forging a sustainable synthesis between contemporary digital fabrication techniques and traditional earthen materials and compositions [23,24].

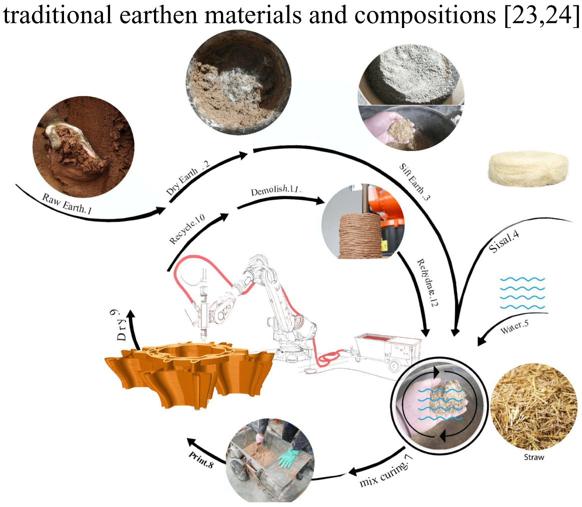

Fig.1. Perception of the continuous construction of buildings using minimally processed earth with employing 3D printing, it embodies a circular building process [Diagram adapted from: https://doi.org/10.1016/j.conbuildmat.2024.135714].

3.1. Material Sourcing

The initial phase of any extensive earthen construction endeavor encompasses the procurement of soil comprising an optimal blend of clay and sand. Termed as "sandy clay loam," soil consisting of approximately 30% clay and 70% sand presents a favorable combination of malleability, minimal shrinkage, and bonding properties, these types of soils are widely available, and straightforward tactics can be implemented to expedite the soil-sourcing procedure [20], Identify and study indigenous earthen architectural structures within the vicinity; the most suitable soil materials can typically be sourced locally, and property owners or builders may be amenable to providing guidance as shown in Fig.2. The appearance and consistency of soil in indigenous earth constructions can serve as a visual reference point during geological assessments for high-quality construction resources. Traverse alluvial plains to uncover potential earth construction resources. Beneath an upper layer of nutrient-rich soil enriched with organic matter lies a stratum of inorganic silt, sand, and clay that prove optimal for earthen construction endeavors. Explore regions situated at the base of eroded mountain ranges, which are known to yield viable sources of soil for construction purposes. These locations, prone to erosion, are susceptible to sediment deposition following periodic flooding events, resulting in silty soils readily available on the surface of seasonal riverbeds.

Fig.2. Earth material "Ecoclay" sourcing process sourced from Valldaura – Spain.

In the field, a seasoned earth construction expert can effectively evaluate the soil's suitability for building purposes through a tactile exploration involving the addition of water to assess texture, cohesion, and clay content manually with existing research and construction manuals propose various on-site testing methods to enhance the reliability and objectivity of these somewhat subjective assessments which Plasticity and cohesion levels can be gauged by molding wet soil into either a ball or a rope, providing an estimation of the clay content present also Local builders are well-acquainted with the characteristics of the material, commonly referred to as "Montecito mud," an alluvial soil rich in clay and devoid of organic components [25].

3.2. Material Processing

In the process of 3DP earthen materials, local soil is initially subjected to processing to ensure its compatibility with the specific project requirements and extrusion system utilized. Earth possessing an optimal earth-to-sand ratio should be identified through testing. The material undergoes a sieving process to eliminate large rocks and organic debris that are unsuitable for pumping purposes or do not align with the characteristics of the extrusion system as shown in Fig.3. For all experiments detailed subsequently, the earth underwent air-drying and sieving through a 2 mm screen. While moist soil can undergo sieving, its tendency to clump may diminish the yield, thus emphasizing the preference for a dry mixture. where available, industrial soil sieving machinery like conveyor-fed shake tables can be employed to expedite the process, particularly for enhancing throughput. After sieving, the earth is combined with water and any essential additives, such as chopped straw, sisal, or supplementary sand, to create a blend that is both extrudable and performance-oriented. Post-mixing, it is deemed ideal for the earthen material to rest for 24 hours, facilitating complete clay hydration and homogenization, thereby mitigating inconsistencies in the extrusion phase prompted by material variations. Well-prepared material is subsequently loaded into the extrusion mechanism, marking the commencement of the printing process [26].

Fig.3. Earth-based composite process of hydration and homogenization

3.2.1. Fibre and additives

The formulation of earthen materials intended for 3D printing can be adapted utilizing principles akin to those governing rammed earth, cob, or rammed earth construction techniques, and the adjustment of various mixing parameters holds the potential to enhance mechanical performance, while the inclusion of binders can be employed to augment compressive strength and durability. Augmentation of sand or aggregate content serves to mitigate contraction, whereas the addition of higher clay proportions enhances cohesion and plasticity moreover, The incorporation of natural fibers such as straw or sisal is conducive to promoting uniform drying and bolstering overall structural integrity within the determination of an optimal distribution of fiber size and quantity emerges as a stimulating frontier for pioneering endeavors, especially pertinent in regions with high moisture levels as seen in Northern Europe or Asia, also the preliminary processing of straw involves rough chopping to generate fibers spanning lengths as shown in Fig.4 from 10 mm to 100 mm which in cases where sisal fibers are shorter than the diameter of the extrusion nozzle, their alignment within the extruded material remains stochastic, while fibers surpassing the nozzle diameter assume an aligned disposition within the pumping system [21].

The deployment of aligned fibers sometimes hinders their contact with the print surface, thereby diminishing the efficacy of hollow fibers like straw or sisal in achieving uniform drying and sustained moisture control. An increased percentage of sisal content has demonstrated advantages in enhancing cohesion stability, achieving uniform crack-free contraction-enhanced ductility, and bolstering compressive strength, underpinning prior investigations by Koutous [21] in the domain of rammed-earth construction. However, the electromechanical extrusion system employed encountered challenges in consistently accommodating an 'ideal' fiber ratio of 5-15% by weight. Initial experimentation was conducted utilizing a weight proportion of 10% straw or sisal content.

Fig.4. Sisal and straw fiber additives length (0.5-1)cm maximum size

3.2.2. Extruding system

This research segment delves into the additive manufacturing capacity of various earth-derived composites by producing scaled cylindrical structures measuring 10 cm in diameter and 20 cm in height. The study involves the assessment of two nozzle diameters (15mm and 20mm) utilizing an advanced RAM extrusion system as shown in Fig.5 developed by 3D Potter®. Two distinct clay varieties were employed in constituting the fundamental components of these composites, namely earthenware "Ecoclay". A binder in the form of sodium silicate was incorporated during the mixing and extrusion phases to bolster the cohesion and strength of the constituents as shown in Fig.5 optimum developed composition, thereby facilitating improved formability and structural resilience.

3.3. Life cycle assessment

Although raw earth possesses inherent recyclability, the processing, manufacturing, and eventual deconstruction of a 3D-printed earth structure do introduce environmental considerations. At present, the absence of inhabited or demolished 3D-printed earth buildings that have subsequently undergone recycling precludes the possibility of conducting a comprehensive Life Cycle Assessment (LCA) encompassing operational energy expenses or end-of-life outcomes. Nonetheless, it is feasible to conduct a cradle-to-cradle life cycle assessment of a test print by referencing established methodologies for assessing the life cycle of earth-based architectural constructions.

Energy outlays associated with processing, water utilization, and fabrication, can be interlinked with the volume of extruded material as shown in Fig.5, a metric directly derived from the digital blueprint of the 3D printing toolpath and the volume of the composite's constituent cubes (measuring 5x5x5cm) as shown in Fig.5. This approach yields an evaluation of the embodied carbon cost per meter of extrusion applicable to the specific Large-Scale Additive Manufacturing (LSAM) configuration employed. Subsequently, the carbon footprint of a functional unit of 3D-printed earth can be quantified based on a per kilogram model, alongside a volumetric comparison against conventional building materials [27].

Fig.5. An investigation into various earth-based compositions, molded into standard 5x5x5cm cubes as detailed in the results section. This explains the utilization of different ingredients to enhance mechanical strength while minimizing embodied carbon.

The 2019 Infrastructure Carbon Emissions Database (ICE), Ecoinvent, and the forthcoming 2023 Carbon Leadership Forum's North American Material Baseline report are consulted to establish a meaningful benchmark for comparing the environmental impact of 3D-printed earth constructions with prevalent construction materials available in the market.

3.4. Compressive Strength

The LR50K Plus, shown in Fig.6, is a powerful compression testing machine that is capable of generating compressive forces up to 50kN. It is a reliable and precise machine that is used extensively in the construction and engineering industries to test the compressive strength of various materials such as concrete, bricks, and metals, When using the LR50K Plus machine, the test samples were placed between two compression plates and a compressive force is applied at a constant rate until the sample either fractures or deforms. The machine carefully records the amount of force required to crush the sample, and this information is analyzed using the software Nexygen.

Fig.6. Compressive load testing using LR50K Plus along with real-time tracking software Nexygen.

The Nexygen software is a powerful tool that is used to collect and analyze test data. It provides a range of features that make compressive strength testing more efficient, such as real-time monitoring of test data, automatic calculation of test results, and easy reporting of test results.

The output of this test was the compressive force/ load (P) measured in Newton(N) to further calculate the compressive strength the mentioned below formula was used.

$$F = P/A \quad (1)$$

Where:
F = The compressive strength (MPa)
P = Maximum load (failure load) applied to the specimen (N)
A = Cross-sectional area of the specimen resisting the load (mm2)

Using this formula all the samples were calculated for their compressive strengths (Table 1) and compared and analyzed in the test results section.

Table 1. Compressive strengths and forces for the composites

Composite Code	N/mm^2	MPa
P3	2322	0.93
P4	3700	1.5
P5	616	0.25
P6	3790	1.516
P7	6600	2.64
P8	2570	1.028
P9	1029	0.411

4 Results and Discussion

In the study, a total of nine composites (P1-P9) were prepared and tested for their compressive strengths. Among these, composites P3-P9 exhibited promising compressive strengths, with P7 demonstrating the highest compressive strength, followed by P6 and P4. On the other hand, P5, P9, and P3 displayed the weakest strengths. To further evaluate the environmental impact of these composites, the embodied carbon (EC) of each composite was calculated. The embodied carbon values were then utilized to assess the Global Warming Potential (GWP) of each composite as shown in Tables 5-13, with a focus on identifying environmentally suitable options for digital fabrication. From the graph depicting the embodied carbon of each composite, it is evident that composites P4, P8, and P7 showcased the lowest values at 13.96 KgCO_2E, 15.46 KgCO_2E, and 17.11 KgCO_2E, respectively as shown in Fig.7. This indicates that these particular composites have a relatively lower environmental impact in terms of carbon emissions. These findings are significant as they highlight the potential for using these composites in digital fabrication processes as shown in Tables 2-4, not only due to their favourable compressive strengths but also because of their lower environmental footprint. These results suggest that a careful selection of composites based on both mechanical properties and environmental impact can lead to the development of more sustainable materials for various applications.

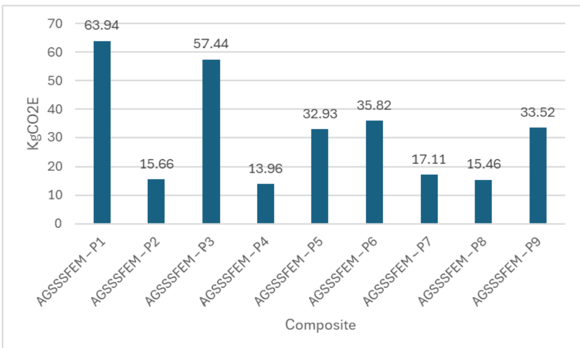

Fig.7. Embodied carbon values of the earth-based compositions

Table 2. Earth-based compositions material matrix (P1, P2, P3).

g/cm^3									
Composition Code	Material	AGSSSFEM – **P1**	%	Material	AGSSFEM – **P2**	%	Material	AGSSFEM – **P3**	%
A1-Earth	**EC**	350g	70	**EC**	350g	70	**EC**	350g	70
A2-Aggregate	**FS**	125g	25	**FS**	125g	25	**FS**	125g	25
A3-Fiber	**Sisal**	25g	5	**Cryp**$_{x<<1mm}$	25g	5	**Sisal**	25g	5
% sum	**500g**		**100**	**500g**		**100**	**500g**		**100**
B1-Binder	**SSS**	75g	15	**SSS**	75g	15	**SSL**	115g	23
B2-Stabilizer	**AG**	50g	10	**AG**	50g	10	**AG**	50g	10
Additive Sum	**125g**		**25**	**125g**		**25**	**165g**		**33**
Water	**W**	**125g**	20	**W**	125g	20	**W**	133g	20
Total material Mass	**625g**		Sum	**625g**		Sum	**665g**		Sum
One cube (5x5x5)cm Total Volume **T.V** Composition Density **C. D**		**125 cm3 0.547g/cm^3**	**125**	**125 cm3 0.135g/cm^3**		**125**	**125 cm3 0.547g/cm^3**		**133**

Table 3. Earth-based compositions material matrix (P4, P5, P6).

g/cm^3									
Composition Code	Material	AGSSSFEM – **P4**	%	Material	AGSSFEM – **P5**	%	Material	AGSSFEM – **P6**	%
A1-Earth	**EC**	350g	70	**EC**	350g	70	**EC**	350g	70
A2-Aggregate	**FS**	125g	25	**BA**	165g	25	**BA**	165g	25
A3-Fiber	**Cryp**$_{x<<1mm}$	25g	5	**Cryp**$_{x<4mm}$	52.5g	10	**Cryp**$_{x<<4mm}$	25g	10
% sum	**500g**		**100**	**500g**		**105**	**500g**		**105**
B1-Binder	**SSL**	115g	23	**SSS**	80g	15	**SSL**	110g	20
B2-Stabilizer	**AG**	50g	10	**AG**	52.5g	10	**AG**	52.5g	10
Additive Sum	**165g**		**33**	**125g**		**25**	**165g**		**30**
Water	**W**	150 g	20	**W**	145g	20	**W**	150g	20
Total material Mass	**665g**		Sum	**625g**		Sum	**665g**		Sum
One cube (5x5x5)cm Total Volume **T.V** Composition Density **C. D**		**125 cm^3 0.135g/cm^3**	**125**	**125 cm^3 0.132g/cm^3**		**125**	**125 cm^3 0.132g/cm^3**		**133**

Table 4. Earth-based compositions material matrix (P7, P8, P9).

g/cm^3									
Composition Code	Material	AGSSSFEM – **P7**	%	Material	AGSSFEM – **P8**	%	Material	AGSSFEM – **P9**	%
A1-Earth	**EC**	385g	70	**EC**	385g	70	**EC**	385g	70
A2-Aggregate	**LM**	165g	30	**LM**	165g	30	**BA**	165g	30
A3-Fiber	**Cryp**$_{x<<4mm}$	55g	10	**Cryp**$_{x<<1mm}$	55g	10	**Cryp**$_{x<<4mm}$ **Sisal**	55g 55g	10 10
% sum	**605g**		**110**	**605g**		**110**	**660g**		**120**
B1-Binder	**SSS**	82.5g	15	**SSL**	110g	20	**SSL**	110g	20
B2-Stabilizer	**AG**	55g	10	**AG**	55g	10	**AG**	55g	10
Additive Sum	**137.5g**		**25**	**165g**		**30**	**165g**		**30**
Water	**W**	150 g	20	**W**	154g	20	**W**	165g	20
Total material Mass	**742.5g**		Sum	**770g**		Sum	**825g**		Sum
One cube (5x5x5)cm Total Volume **T.V** Composition Density **C. D**		**125 cm^3 0.126g/cm^3**	**135**	**125 cm^3 0.126g/cm^3**		**140**	**125 cm^3 0.121g/cm^3**		**150**

Table 5. Embodied carbon calculations for earth-based composition P1.

Composition Code	Material	% in 1 Tn	Quantity in Kg	Density Kg/m^3	GWP kgCo2E/ kg	Kg/m2 Thickness 0.25m	Embodied carbon $KgCO_2e/m^2$
AGSSSFEM – **P1**	Eco-clay	70	700kg	1810	0.423	95.72	40.5
	Fine sand	25	250kg	1670	0.004	34.2	0.14
	Sisal	5	50kg	1500	0.132	6.83	0.90
Density Kg/m^3	Sodium silicate solid	15	150kg	1200	0.55	20.51	11.3
547	Arabic gum	10	100kg	630	0.81	13.7	11.1
Sum						**136.75**	**63.94**

Table 6. Embodied carbon calculations for earth-based composition P2.

Composition Code	Material	% in 1 Tn	Quantity in Kg	Density Kg/m^3	GWP $kgCO_2E$/ kg	Kg/m^2 Thickness 0.25m	Embodied carbon $KgCO_2e/m^2$
AGSSSFEM – **P2**	Eco-clay	70	700kg	1810	0.423	23.8	10.06
	Fine sand	25	250kg	1670	0.004	8.5	0.034
	Cryptomeria <<1mm	5	50kg	309	$1.4x10^{-2}$	1.7	0.023
Density Kg/m^3	Sodium silicate solid	15	150kg	1200	0.55	5.1	2.80
136	Arabic gum	10	100kg	630	0.81	3.4	2.75
Sum						**34**	**15.667**

Table 7. Embodied carbon calculations for earth-based composition P3.

Composition Code	Material	% in 1 Tn	Quantity in Kg	Density Kg/m3	GWP $kgCO_2E$/ kg	Kg/m^2 Thickness 0.25m	Embodied carbon $KgCO_2e/m^2$
AGSSSFEM – **P3**	Eco-clay	70	700kg	1810	0.423	95.72	40.5
	Fine sand	25	250kg	1670	0.004	34.2	0.14
	Sisal	5	50kg	1500	0.132	6.83	0.90
Density Kg/m^3	Sodium silicate Liquid	23	230kg	1530	0.150	31.7	4.8
547	Arabic gum	10	100kg	630	0.81	13.7	11.1
Sum						**136.75**	**57.44**

Table 8. Embodied carbon calculations for earth-based composition P4.

Composition Code	Material	% in 1 Tn	Quantity in Kg	Density Kg/m3	GWP $kgCO_2E$/ kg	Kg/m^2 Thickness 0.25m	Embodied carbon $KgCO_2e/m^2$
AGSSSFEM – **P4**	Eco-clay	70	700kg	1810	0.423	23.625	9.99
	Fine sand	25	250kg	1670	0.004	8.437	0.033
	Cryptomeria<< 4mm	5	50kg	309	$1.4x10^{-2}$	1.7	0.023
Density Kg/m^3	Sodium silicate Liquid	23	230kg	1530	0.150	7.8	1.17
135	Arabic gum	10	100kg	630	0.81	3.4	2.75
Sum						**33.75**	**13.966**

Table 9. Embodied carbon calculations for earth-based composition P5.

Composition Code	Material	% in 1 Tn	Quantity in Kg	Density Kg/m^3	GWP $kgCO_2E$/ kg	Kg/m^2 Thickness 0.25m	Embodied carbon $KgCO_2e/m^2$
AGSSSFEM – **P5**	Eco-clay	70	700kg	1810	0.423	23.1	9.77
	Basalt	25	250kg	1240	2.39	8.25	19.71
	Cryptomeria<<4 mm	10	50kg	309	$1.4x10^{-2}$	3.3	0.046
Density Kg/m^3	Sodium silicate Liquid	15	150kg	1530	0.150	4.95	0.742
132	Arabic gum	10	100kg	630	0.81	3.3	2.67
Sum						**33**	**32.938**

Table 10. Embodied carbon calculations for earth-based composition P6.

Composition Code	Material	% in 1 Tn	Quantity in Kg	Density Kg/m^3	GWP $kgCO_2E/kg$	Kg/m^2 Thickness 0.25m	Embodied carbon $KgCO_2e/m^2$
AGSSSFEM – **P6**	Eco-clay	70	700kg	1810	0.423	23.1	9.77
	Basalt	25	250kg	1240	2.39	8.25	19.71
	Cryptomeria<<4mm	10	50kg	309	$1.4x10^{-2}$	3.3	0.046
Density Kg/m^3	Sodium silicate solid	20	200kg	1200	0.55	6.6	3.63
132	Arabic gum	10	100kg	630	0.81	3.3	2.673
Sum						**33**	**35.829**

Table 11. Embodied carbon calculations for earth-based composition P7.

Composition Code	Material	% in 1 Tn	Quantity in Kg	Density Kg/m^3	GWP $kgCO_2E/kg$	Kg/m^2 Thickness 0.25m	Embodied carbon $KgCO_2e/m^2$
AGSSSFEM – **P7**	Eco-clay	70	700kg	1810	0.423	22.05	9.327
	lime	30	300kg	2700	0.275	9.45	2.598
	Cryptomeria<<4mm	10	100kg	309	$1.4x10^{-2}$	3.15	0.044
Density Kg/m^3	Sodium silicate solid	15	150kg	1200	0.55	4.725	2.598
126	Arabic gum	10	100kg	630	0.81	3.15	2.551
Sum						**31.5**	**17.118**

Table 12. Embodied carbon calculations for earth-based composition P8.

Composition Code	Material	% in 1 Tn	Quantity in Kg	Density Kg/m^3	GWP $kgCO_2E/kg$	Kg/m^2 Thickness 0.25m	Embodied carbon $KgCO_2e/m^2$
AGSSSFEM – **P8**	Eco-clay	70	700kg	1810	0.423	22.05	9.327
	lime	30	300kg	2700	0.275	9.45	2.598
	Cryptomeria<<1mm	10	100kg	309	$1.4x10^{-2}$	3.15	0.044
Density Kg/m^3	Sodium silicate Liquid	20	200kg	1530	0.150	6.3	0.945
126	Arabic gum	10	100kg	630	0.81	3.15	2.551
Sum						**31.5**	**15.465**

Table 13. Embodied carbon calculations for earth-based composition P9.

Composition Code	Material	% in 1 Tn	Quantity in Kg	Density Kg/m^3	GWP $kgCO_2E/kg$	Kg/m^2 Thickness 0.25m	Embodied carbon $KgCO_2e/m^2$
AGSSSFEM – **P9**	Eco-clay	70	700kg	1810	0.423	21.175	8.957
	Basalt	30	300kg	1240	2.39	9.075	21.68
	Cryptomeria<<4mm	10	100kg	309	$1.4x10^{-2}$	3.025	0.042
	Sisal	10	100kg	1500	0.132	3.025	0.399
Density Kg/m^3	Sodium silicate solid	20	200kg	1200	0.55	6.05	
121	Arabic gum	10	100kg	1500	0.81	3.025	2.450
Sum						**30.25**	**33.528**

5 Remark conclusion

In this research, we explored the use of diverse earth-based composites in additive manufacturing, significantly enhancing their workability and engineering qualities. This improvement was achieved through the strategic integration of solid and liquid sodium silicate binders. Notably, Arabic gum, derived from the acacia tree, proved to be a pivotal substance for earth stabilization and ingredient bonding, even in small amounts. Acting as a primary flocculant, Arabic gum develops cohesive flocs, binding clay particles within the earth matrix to significantly enhance dry compressive strength while reducing water absorption and shrinkage. However, its solubility in water limits prolonged moisture protection. To maximize the advantages of Arabic gum, which is effective at 1.5% to 3%, complementary natural elements such as sisal and cryptomeria fibers are essential. These natural fibers reinforce the composite, bolstering its overall structural integrity. Additionally, the inclusion of natural lime in the composition significantly increased mechanical resistance, as evidenced by the enhanced compressive strength. Combined with fine sand, stone dust aggregates, and basalt, this composite achieves a well-balanced synergy, blending mechanical reinforcement benefits with stabilizing properties as show in Fig.6, and Fig.7. It is important to note that Arabic gum concentrations above 3%, as observed in composites P1 and P2, increase viscosity, making the composite hard to control in the casting process but easier to extrude with an electromechanical extruder system. The embodied carbon results of the composition, discussed in the Results and Discussion sections, further validate our findings. The use of natural fibers and earth-based materials not only enhances mechanical strength but also offers a sustainable approach to construction by reducing the carbon footprint compared to traditional building materials. In conclusion, this research provides compelling evidence that the integration of Arabic gum, natural lime, and natural fibers as sisal into earth-based composites significantly enhances their structural and environmental performance. These findings pave the way for future investigations into sustainable construction materials, ultimately advancing eco-friendly building practices in the field of additive manufacturing.

This research was funded by Minho University and Lab2PT (Landscapes, Heritage, and Territory Laboratory) through a Doctoral Grant from the Foundation for Science and Technology (FCT), reference number 2021/07670/BD. The Institute of Design of Guimarães provided hosting and support for the Advanced Ceramics R&D Lab and ARENA LAB, offering access to their facilities and equipment necessary for conducting research tests and developing prototypes.

References

1. J. Assunção, K ChadhaL. Vasey, C. Brumaud, and G. Habert (2023). Can digital fabrication meet low-carbon materials? A closer look at the environmental impact of 3D printing with earth. ETH Zurich. https://doi.org/10.3929/ETHZ-B-000640421
2. K.Kuzmenko, A. Feraille, O. Baverel, N. Roussel. Environmental Impacts of 6-Axes Robotic Arm for 3D Concrete Printing, in: Bos, F.P., Lucas, S.S., Wolfs, R.J.M., Salet, T.A.M. (Eds.), Second RILEM International Conference on Concrete and Digital Fabrication, RILEM Bookseries. Springer International Publishing, Cham, pp. 1023–1030. https://doi.org/10.1007/978-3-030-49916-7_99(2020).
3. V. Voney, P. Odaglia, C. Brumaud, B. Dillenburger, G. Habert. From casting to 3D printing geopolymers: A proof of concept. Cem. Concr. Res. 143. https://doi.org/10.1016/j.cemconres.2021.106374(2021).
4. F. Boscaro, E. Quadranti, T. Wangler, S. Mantellato, L. Reiter, R.J. Flatt. Eco-Friendly, Set-on-Demand Digital Concrete. 3D Print. Addit. Manuf. 9, 3–11. https://doi.org/10.1089/3dp.2020.0350(2022).
5. A. Perrot, D. Rangeard, E. Courteille. 3D printing of earth-based materials: Processing aspects. Constr. Build. Mater. 172, 670–676. https://doi.org/10.1016/j.conbuildmat.2018.04.017 (2018).
6. M.R.M. Saade, A. Yahia, B. Amor. How has LCA been applied to 3D printing, Asystematic literature review and recommendations for future studies. J. Clean. Prod. 244, 118803. https://doi.org/10.1016/j.jclepro.2019.118803(2020).
7. A. Perrot, D. Rangeard, F.Menasria, S. Guihéneuf. Strategies for optimizing the mechanical strengths of raw earth-based mortars. Constr. Build. Mater. https://doi.org/10.1016/j.conbuildmat.2018.02.055 (2018).
8. H. Alhumayani, M. Gomaa, V. Soebarto, W. Jabi. Environmental assessment of large-scale 3D printing in construction: A comparative study between cob and concrete. J. Clean. Prod. 270, 122463. https://doi.org/10.1016/j.jclepro.2020.122463(2020).
9. M. Gomaa, S. Schade, D.W. Bao, Y.M. Xie. Automation in rammed earth construction for industry 4.0: Precedent work, current progress, and future prospect. J. Clean. Prod. 398, 136569. https://doi.org/10.1016/j.jclepro.2023.136569(2023).
10. A. Ofer, B. Arnon, P. Larianovsky, A. Sprecher, From soil to printed structures: a systematic

approach to designing clay-based materials for 3D printing in construction and architecture, Constr. Build. Mater. 408 (December) 133783, https://doi.org/10.1016/j.conbuildmat.2023.133783 (2023).

11. IAAC and WASP: new 3D printing strategies towards the realisation of load-bearing earthen structures, IAAC (Blog) May 29, https://iaac.net/iaac-wasp-new-3d-printing-strategies-towards-realisation-load-bearing-earthen-structures(2019).
12. G. Giuffrida, R. Caponetto and M. Cuomo (2019). An overview on contemporary rammed earth buildings: technological advances in production, construction and material characterization. In IOP Conference Series: Earth and Environmental Science (Vol. 296, Issue 1, p. 012018). IOP Publishing. https://doi.org/10.1088/1755-1315/296/1/012018
13. M. Röck, M. R. M. Saade, M. Balouktsi, F. N. Rasmussen, H. Birgisdottir, R. Frischknecht, G. Habert, T. Lützkendorf and A. Passer (2020). Embodied GHG emissions of buildings – The hidden challenge for effective climate change mitigation. In Applied Energy (Vol. 258, p. 114107). Elsevier BV. https://doi.org/10.1016/j.apenergy.2019.114107
14. M. Bechthold, Z. Seibold and S. Mhatre (2022). Post-tensioned ceramic structures: design, analysis and prototyping. In Architecture, Structures and Construction (Vol. 2, Issue 1, pp. 165–182). Springer Science and Business Media LLC. https://doi.org/10.1007/s44150-022-00025-0
15. B. Khoshnevis (2004). Automated construction by contour crafting—related robotics and information technologies. In Automation in Construction (Vol. 13, Issue 1, pp. 5–19). Elsevier BV. https://doi.org/10.1016/j.autcon.2003.08.012
16. M. Moretti (2023). WASP in the Edge of 3D Printing. In 3D Printing for Construction with Alternative Materials (pp. 57–65). Springer International Publishing. https://doi.org/10.1007/978-3-031-09319-7_3
17. V. Revilla-Cuesta, L. Evangelista, J. de Brito, M. Skaf and J. M. Manso (2022). Shrinkage prediction of recycled aggregate structural concrete with alternative binders through partial correction coefficients. In Cement and Concrete Composites (Vol. 129, p. 104506). Elsevier BV. https://doi.org/10.1016/j.cemconcomp.2022.104506
18. M. Gomaa, W. Jabi, A. Veliz Reyes and V. Soebarto. (2021). 3D printing system for earth-based construction: Case study of cob. In Automation in Construction (Vol. 124, p. 103577). Elsevier BV. https://doi.org/10.1016/j.autcon.2021.103577
19. E. Ferretti, M. Moretti, A. Chiusoli, L. Naldoni, F. De Fabritiis and M. Visonà (2022). Mechanical Properties of a 3D-Printed Wall Segment Made with an Earthen Mixture. In Materials (Vol. 15, Issue 2, p. 438). MDPI AG. https://doi.org/10.3390/ma15020438
20. M. C. Jiménez Delgado and I. C. Guerrero (2007). The selection of soils for unstabilised earth building: A normative review. In Construction and Building Materials (Vol. 21, Issue 2, pp. 237–251). Elsevier BV. https://doi.org/10.1016/j.conbuildmat.2005.08.006
21. A. Koutous and E. Hilali (2021). Reinforcing rammed earth with plant fibers: A case study. In Case Studies in Construction Materials (Vol. 14, p. e00514). Elsevier BV. https://doi.org/10.1016/j.cscm.2021.e00514
22. Compressed Earth Blocks Standards (CDI - CRATerre-EAG, 1998, 144 p.), n.d. Accessed October 10, https://www.nzdl.org/cgi-bin/library?e=d-00000- 00—off-0cdl–00-0——0-10-0—0—0direct-10—4————0–0 l–11-en-50—20- about—00-0-1-00-0-0-11-1-0utfZz-8-10&cl=CL4.30&d=HASH01979938ef89e979ddfb736b&gt=2(2023).
23. C. Roux, K. Kuzmenko, N. Roussel, R. Mesnil and A. Feraille. Life cycle assessment of concrete 3D printing process. Int. J. Life Cycle Assess. 28, 1–15. https://doi.org/10.1007/s11367-022-02111-3.
24. D. Andreau and L. Delboy, World Heritage Inventory of Earthen Architecture, CRATerre-ENSAG, France, (2012). 〈https://unesdoc.unesco.org/ark:/48223/pf0000217020(2023).
25. L. A. Wolfskill, et. al, Handbook for Building Homes of Earth, Washington D.C.: Department of Housing and Urban Development, Division of International Affairs (1969).
26. A. Curth. 3D Printed Earth Formwork for Reinforced Concrete Construction. US Patent Office 63/507,725, filed June 12, (2023).
27. P. Estève, C. Beckett, R. Pedreschi, F. Bosche, J. C. Morel, R. Charef and G. Habert (2022). Developing an integrated BIM/LCA framework to assess the sustainability of using earthen architecture. In IOP Conference Series: Earth and Environmental Science (Vol. 1078, Issue 1, p. 012100). IOP Publishing. https://doi.org/10.1088/1755-1315/1078/1/012100